New prototype multi-gap resistive plate chambers with long strips

Y.J. Sun [a], C. Li [a,*], M. Shao [a], B. Gui [a], Y.E. Zhao [a], H.F. Chen [a], Z.B. Xu [b], L.J. Ruan [b], G.J. Lin [c], X. Wang [d], Y. Wang [d], Z.B. Tang [a], G. Eppley [e], P. Fachini [b], M. Kohl [f], J. Liu [e], W.J. Llope [e], R. Majka [c], T. Nussbaun [e], E. Ramberg [h], T. Sakuma [f], F. Simon [i], N. Smirnov [c], B. Surrow [f], D. Underwood [g]

[a] Department of Modern Physics, University of Science and Technology of China, Hefei 230026, China
[b] Brookhaven National Laboratory, Upton, NY 11973, USA
[c] Yale University, New Haven, CT 06520, USA
[d] Department of Engineering Physics, Tsinghua University, Beijing 100084, China
[e] Rice University, Houston, TX 77251, USA
[f] Massachusetts Institute of Technology, Cambridge, MA 02139-4307, USA
[g] Argonne National Laboratory, Argonne, IL 60439, USA
[h] Fermi National Accelerator Laboratory, Batavia, IL 60510, USA
[i] Max-Planck-Institute for Physics and Excellence Cluster "Universe", Munich, Germany

ARTICLE INFO

ABSTRACT

A new kind of Multi-gap Resistive Plate Chamber (MRPC) has been built for the large-area Muon Telescope Detector (MTD) for the STAR experiment at the Relativistic Heavy Ion Collider (RHIC). These long read-out strip Multi-gap Resistive Plate Chambers (LMRPCs) have an active area of $87.0 \times 17.0\,cm^2$ and ten $250\,\mu m$-thick gas gaps arranged as a double stack. Each read-out strip is 2.5 cm wide and 90 cm long. The signals are read-out at both ends of each strip. Cosmic ray tests indicate a time resolution of $\sim 70\,ps$ and a detection efficiency of greater than 95%. Beam tests performed at T963 at Fermilab indicate a time resolution of 60–70 ps and a spatial resolution of $\sim 1\,cm$ along the strip direction.

1. Introduction

Multi-gap Resistive Plate Chambers (MRPCs) [1,2] are inexpensive gaseous detectors with good timing resolution and high detection efficiency. The readout pads can be shaped into arbitrary shapes to achieve the granularity required in modern heavy-ion collisions. This technology has been chosen for the STAR and PHENIX Time-of-Flight (TOF) systems [3,4] at the Relativistic Heavy Ion Collider (RHIC), the ALICE TOF system [5] at the LHC, to name just a few. If the charged particle multiplicities in the events are not too large, MRPCs with long double-ended read-out strips (LMRPCs) are attractive as these can reduce the number of electronics channels and also provide a measurement of the hit position along each strip via "left minus right" timing.

This LMRPC technology has been selected for the proposed large-area Muon Telescope Detector (MTD) [6] for the STAR experiment. The MTD has been proposed to measure muons of momenta of a few GeV/c. Such a system will allow the detection of di-muon pairs from Quark Gluon Plasma (QGP) thermal radiation, quarkonia, and light vector mesons. The correlation of quarks and gluons as QGP resonances, Drell-Yan production, and the measurement of heavy flavor hadrons via semi-leptonic decays into single muons are also possible. These measurements will advance our knowledge of the nuclear matter formed in the relativistic heavy ion collisions at RHIC. [7] Two LMRPCs were constructed, and have been installed in STAR as a prototype MTD detector. They have successfully taken data since the 2007 run of RHIC. To meet the physics requirements of the MTD, the LMRPCs are required to have a time resolution that is better than 100 ps and a spatial resolution of each hit better than 2 cm. In this paper, the LMRPC prototypes and their performance using both cosmic rays and test beams are described.

2. LMRPC prototype

The LMRPC module has ten gas gaps arranged in a double stack as shown schematically in Fig. 1. The thickness of each gap is $250\,\mu m$ and is defined using a nylon monofilament fishing line. Float glass sheets of 0.7 mm thickness with volume resistivity of $\sim 10^{13}\,\Omega\,cm$ are used as the resistive plates. The positive and the negative high voltage (HV) are applied to an adhesive graphite tape (with surface resistivity of $\sim 200\,k\Omega/\square$) located outside the outermost glass of each stack. The total size of each LMRPC is

* Corresponding author. Tel.: +86 551 3602460; fax: +86 551 3601164.
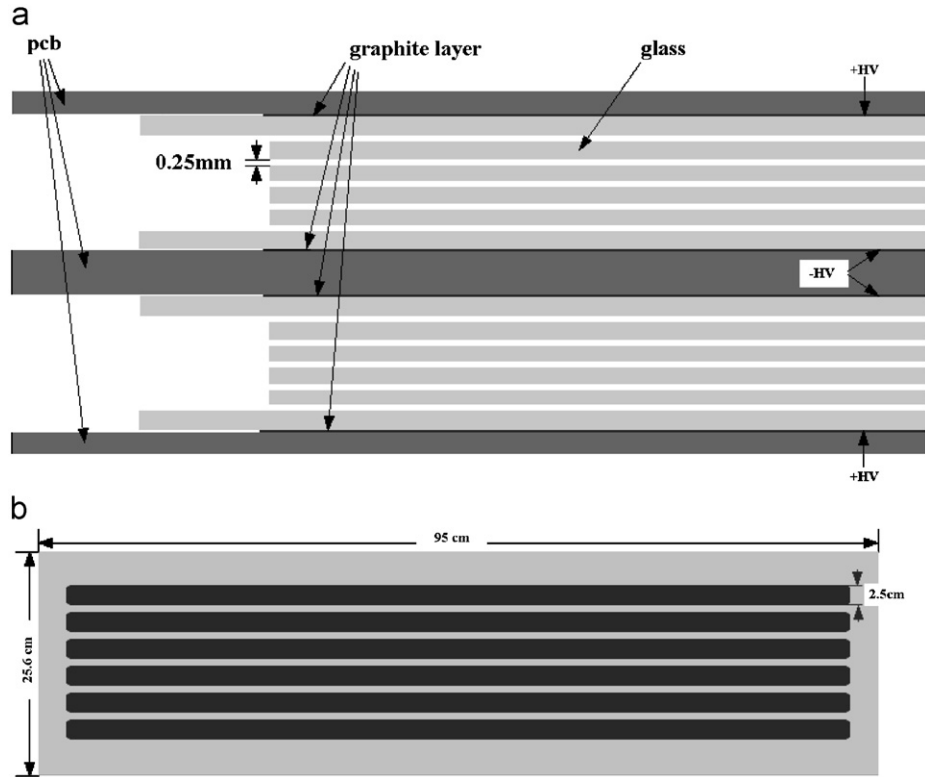E-mail address: licheng@ustc.edu.cn (C. Li).

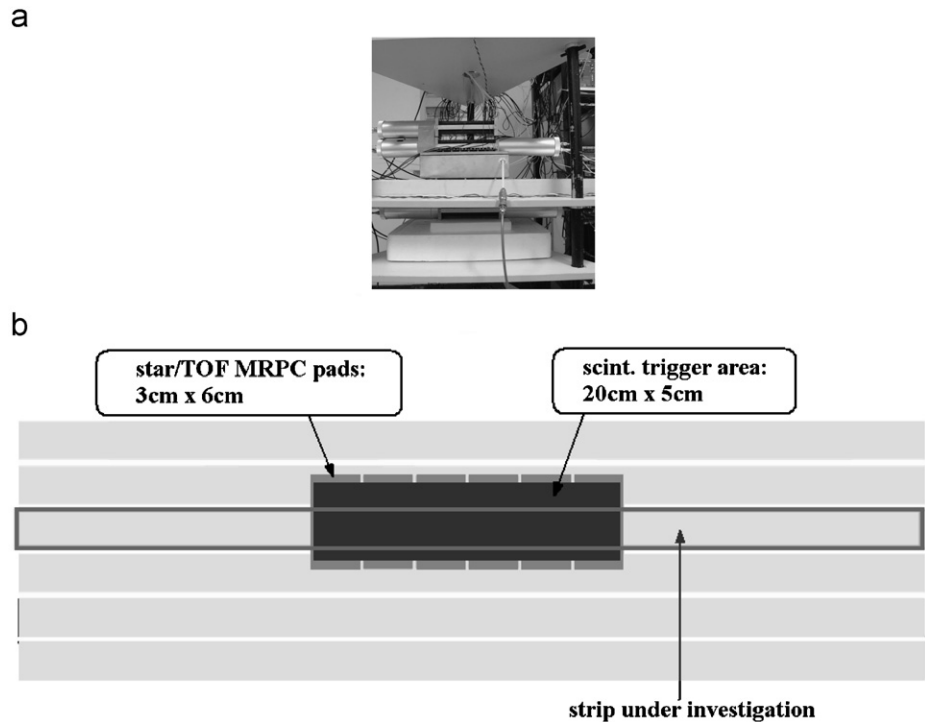**Fig. 1.** Schematic side-view of the LMRPC modules (left frame) and read-out strips (right frame).

Fig. 2. The set-up used for the cosmic ray tests.

$95.0 \times 25.6\,\mathrm{cm}^3$, and the active area defined by the read-out strips is $87.0 \times 17.0\,\mathrm{cm}^2$. The read-out pads are segmented into six double-ended strips which are 2.5 cm wide. The gap between each strip is 4 mm wide. Pins are used to transmit the negative signals from the external strip layers to the central strip layer. Twisted-pair cables bring the differential signals from both ends of the

module to the front-end electronics. These front-end electronics preamplify and amplify the signals and drive the signals into $50\,\Omega$ over long cables to CAMAC ADCs (charge Analog-to-Digital Converter) and TDCs (Time-to-Digital Converter). The thickness of a finished LMRPC is about 3.2 cm, with two pieces of 0.8 cm thick honeycomb boards supporting the whole structure.

The weight of one module is around 7.2 kg. The LMRPC modules are enclosed in a gas-tight aluminum box that is flooded with a mixture of 95% Freon R-134a and 5% iso-butane.

3. Cosmic ray test

The prototype module was tested with cosmic rays using the set-up shown in Fig. 2. Three scintillators were used to define a triggered area of $20.0 \times 5.0 \, cm^2$ along the read-out strips. This trigger area fully covered one LMRPC strip in width (the "strip under investigation") and half each of the two neighboring strips. Two of these scintillators were read-out at both ends with four

fast PMTs which provided the event reference time (T0). A STAR-TOF MRPC module [8] also covered the triggered area with six read-out pads, which divided the triggered area into six segments with an area of $\sim 3 \times 6 \, cm^2$. The LMRPC signals were read-out from both ends via the front-end electronics based on MAXIM 3760 chips. These electronics provided both amplification and discrimination. For additional details on the cosmic tests, see Ref. [9].

The plateau of detection efficiency versus HV is shown in Fig. 3. The detection efficiency is above 95% for positive and negative HV values greater than 6.2 kV. For our subsequent measurements, the positive and negative HV values used were 6.3 kV.

The six pads of the STAR-TOF MRPC gave a rough position information along the read-out strips. Fig. 4 shows the relationship between one-half of the time difference measured from the two ends of the investigated strip and the relative hit position.
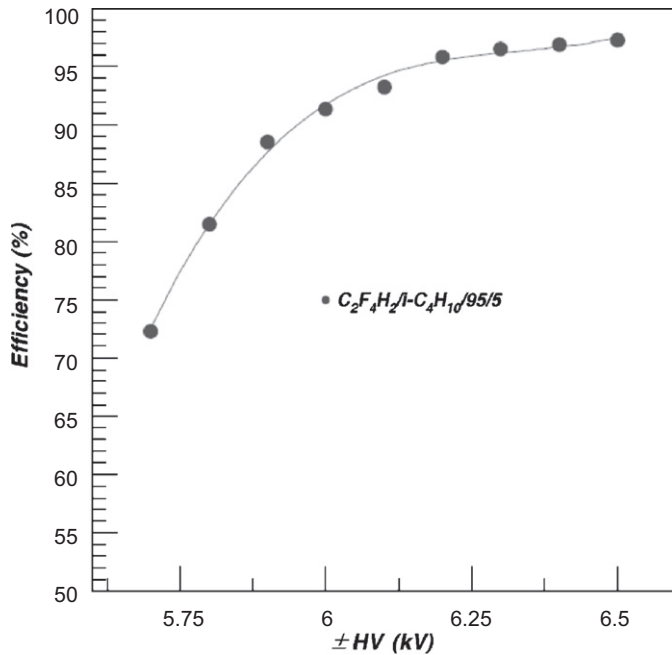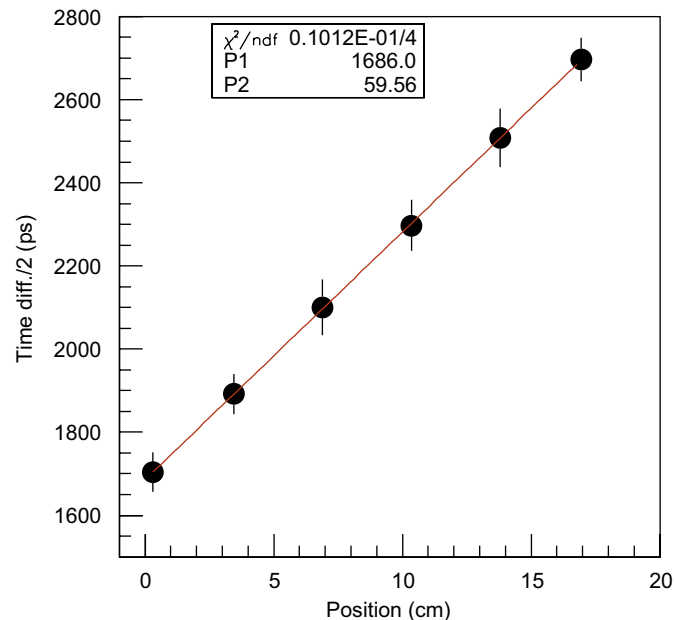

Fig. 3. LMRPC detection efficiency plateau.

Fig. 4. One-half of the time difference measured from the two ends of the investigated strip versus the hit position. The signal propagation velocity along the LMRPC strip is the slope of this line.
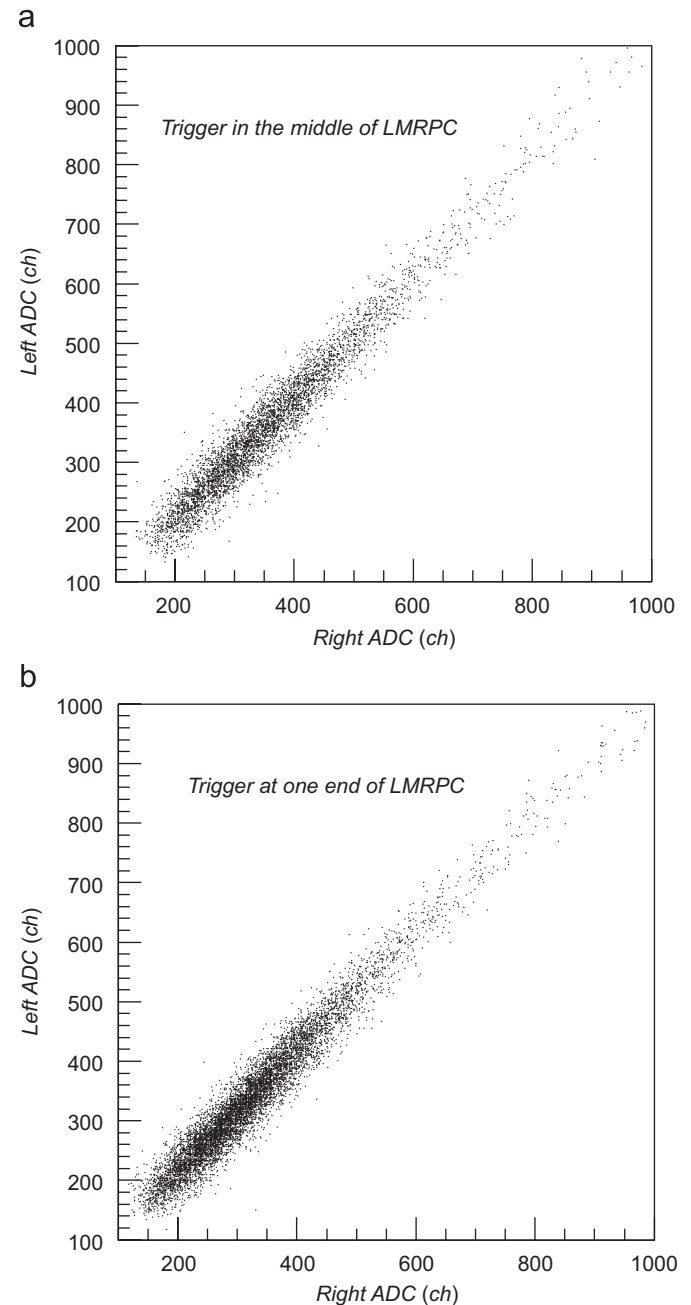

Fig. 5. The correlations of the signal areas from the two ends of one read-out strip for hits near the mid-point (top frame) and one end (bottom frame).

The slope of the linear fit indicates the reciprocal of the signal propagation velocity along the strip, which is observed to be 59.6 ps/cm.

Fig. 5 shows the relationship between the charges of the signals taken from the two ends (left and right) of the read-out strip under investigation. The left frame of this figure shows this relationship when the triggered area was placed in the middle of an LMRPC strip, while the right frame shows this relationship when the triggered area is at an extreme end of the read-out strip. Even in the latter case when the signal-transmitting distances to left and right are quite different, a linear correlation can still be observed. This indicates that the attenuation of pulse area along the strip is neglectable.
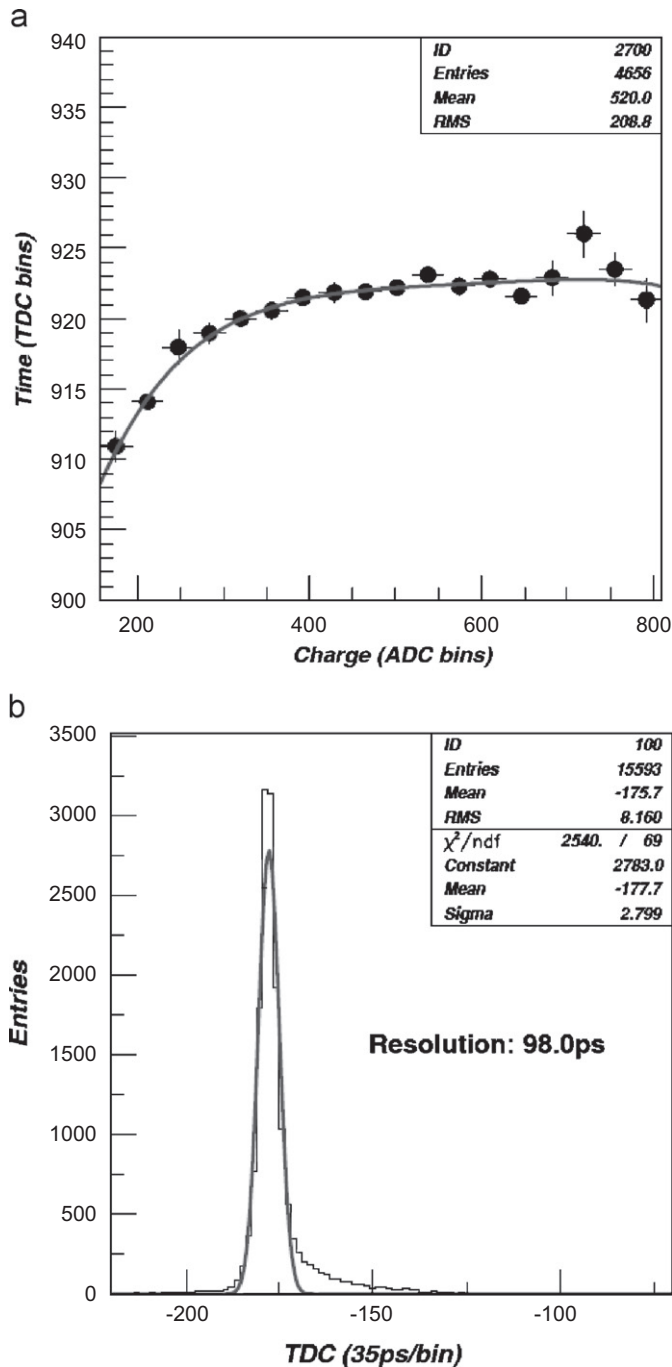
The mean time, $T_{mean} = (T_{left}+T_{right})/2$, formed from the time from the two ends of one strip eliminates the time smearing caused by the position of the hit along the strip. The signals from two ends had been found to be similar in area. Thus, the slewing correction was made between the arithmetical mean of time and pulse area (mT–mA correction), and is shown in Fig. 6a. A sixth-order polynomial was fit to these curves to obtain the slewing correction function. The reference time resolution was 98 ps, as shown in Fig. 6b. The distributions of mean time with respect to the reference time after the mT–mA correction are shown in Fig. 7. Following the subtraction of the reference time resolution in quadrature, the time resolution of the LMRPC itself was observed to be 60 ps (74 ps) when triggered in the middle (at one end) of the module.
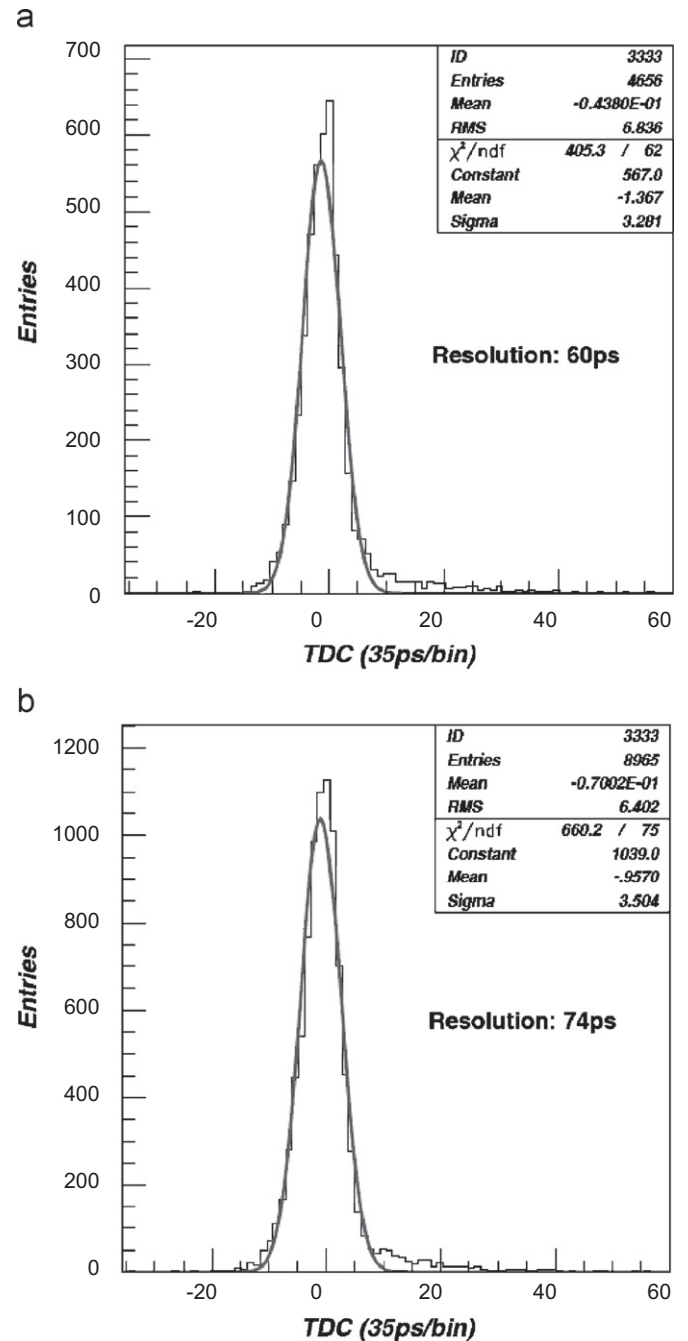
a

b

Fig. 6. The mT–mA slewing correction (top frame) and the resolution of the reference time, T0 (bottom frame).

a

b

Fig. 7. Mean time resolution: (top) trigger in the middle and (bottom) trigger at one end of a strip.
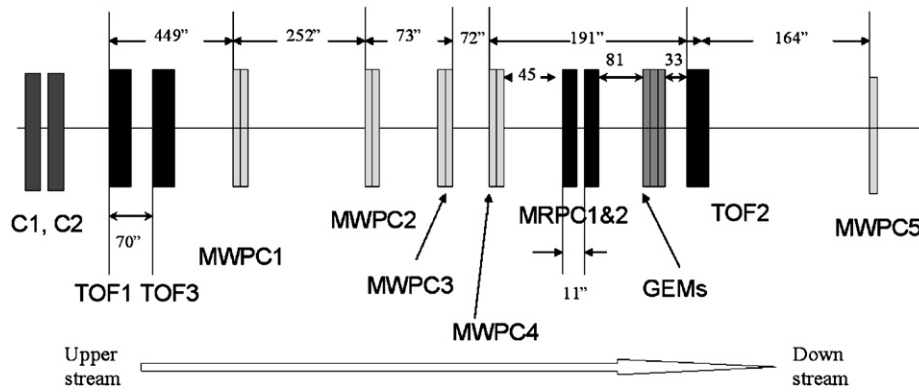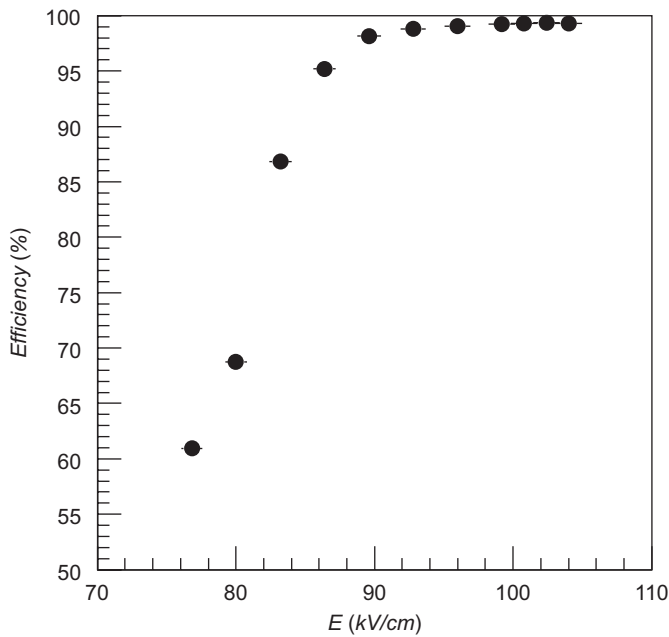
Fig. 8. T963 beam test set-up.

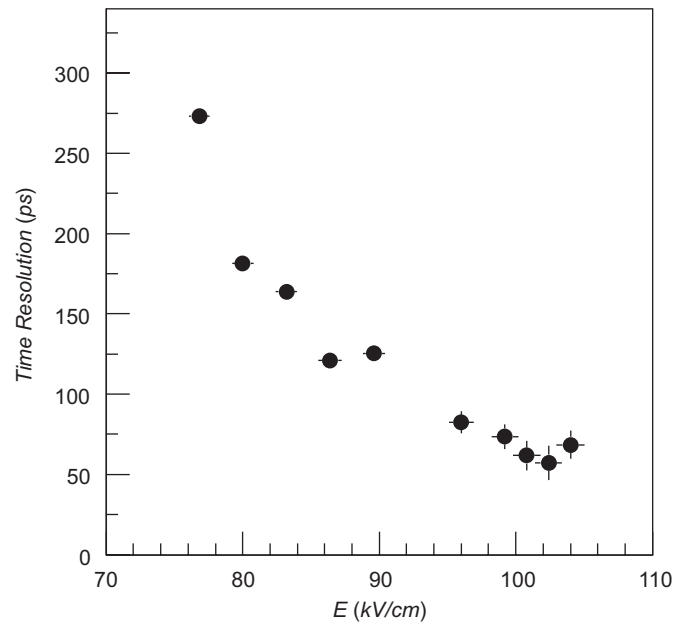**Fig. 9.** Detection efficiency plateau from the beam test.

Fig. 10. Time resolution as a function of electric field.

4. Beam test at FNAL

A beam test experiment (T963) was carried out at the MTEST facility at Fermi National Accelerator Laboratory (FNAL) in May 2007. The beam consisted primarily of 32 GeV muons, pions, and protons. The set-up of the beam test is shown in Fig. 8. Two LMRPC modules were tested. One was made at Tsinghua University (MRPC1, upstream) and the other was made at the University of Science and Technology of China (MRPC2, downstream). These were placed on a movable platform. TOF1, TOF2 and TOF3 are three layers of scintillators. The coincidence of TOF1 and TOF2 was used as the event trigger and the common start signal for the TDCs. TOF3 provided the reference time for the LMRPCs. Nine layers of Multi-Wire Proportional Chambers (MWPCs) and three layers of Gas Electron Multiplier (GEM) chambers provided the beam particle position at the LMRPCs. Two Cherenkov detectors (C1 and C2) were used for beam particle identification.

Fig. 9 shows the detection efficiency plateau of the USTC module. The electric field E in the gas gaps is equal to the applied HV values (the absolute sum of the positive and negative values) divided by the total thickness of all of the gas gaps ($250\,\mu m \times 5$) in one stack. Over a wide range of working electric field values (90–104 kV/cm), the detection efficiency is greater than 98%.

After the slewing correction and the subtraction in quadrature of the reference time resolution, the LMRPC time resolution is plotted versus the electric field and is shown in Fig. 10. The time resolution is less than 70 ps for electric fields between 100–105 kV/cm.

The correlation between the difference of the times measured from the two ends of one LMRPC strip and the particle incident position is shown in Fig. 11. The strong correlation that is observed confirms that the time information can be used to calculate the position of the hit along the strip. The slope of the linear fit indicates a signal propagation velocity of ~60 ps/cm, which is consistent with that obtained from the cosmic ray tests. Shown in Fig. 12a is a scatter-plot of the beam particle position as measured by the GEM detectors versus the LMRPC hit position obtained with the difference of the times at the two ends of one strip. The variance around this correlation, shown in Fig. 12b, is assumed to result purely from the LMRPC spatial resolution and is observed to be of 0.6–1.0 cm since the spatial resolution of GEM is found to be around 70 μm [10].

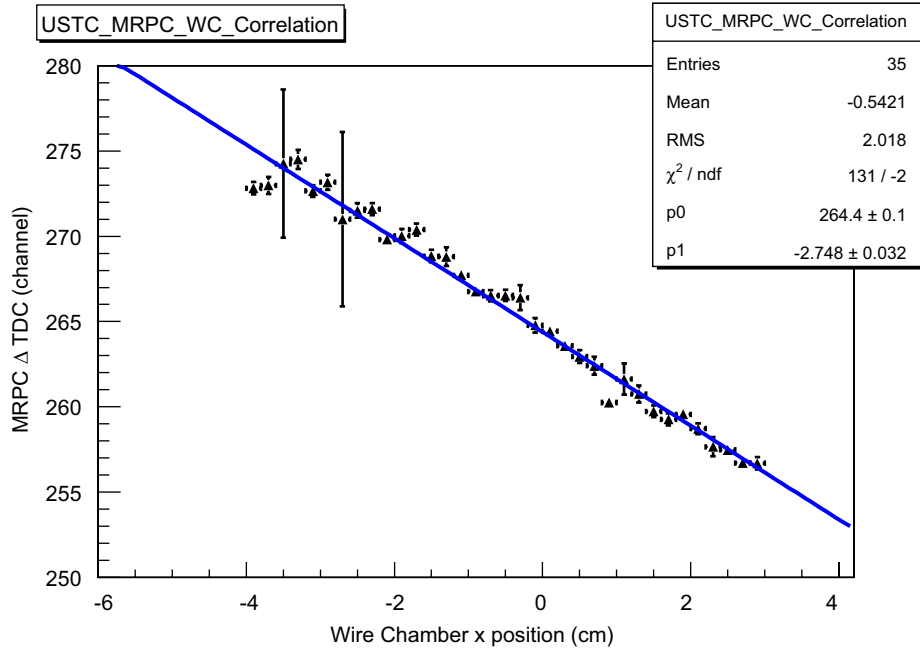**Fig. 11.** Correlation between the LMRPC time difference and charged particle position measured by MWPC.
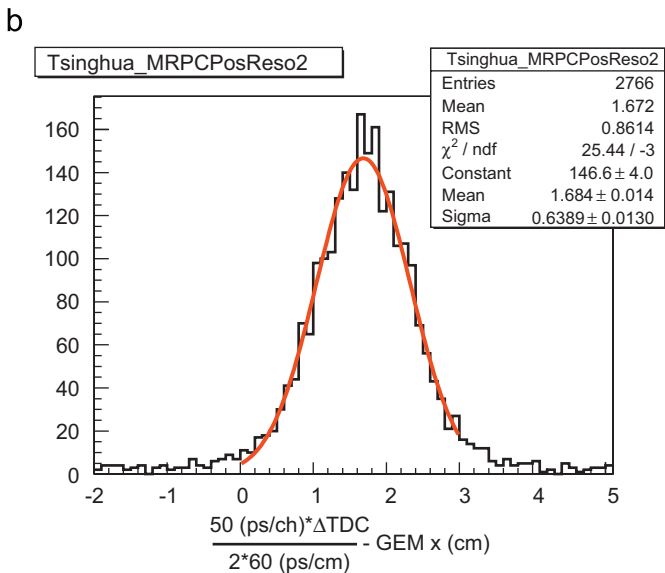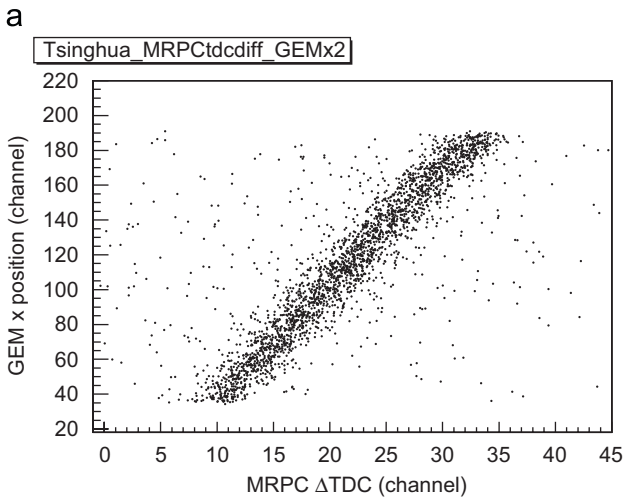
a

b

Fig. 12. (a) The hit position from the GEM chambers versus the hit position from the LMRPC time differences and (b) spatial resolution of LMRPC.
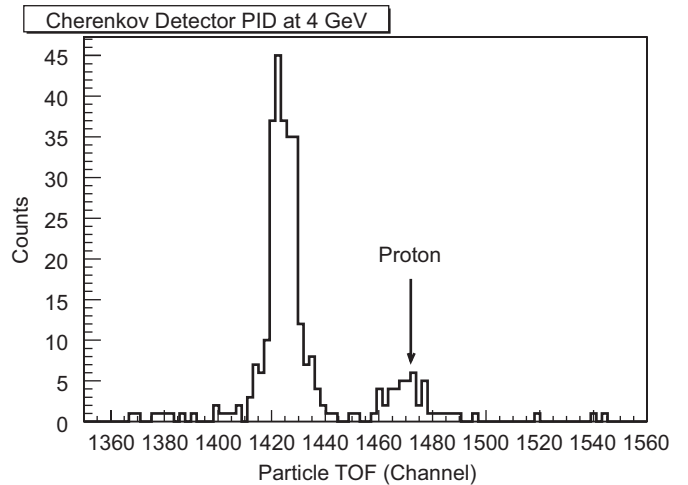

Fig. 13. Proton identification by time of flight measurement of LMRPC.

The beam energy was also tuned down to 4 GeV. The Cherenkov detectors were used to separate protons from pions and muons. At this beam energy and in the present set-up, the TOF of the protons from TOF1 to LMRPC (∼890 in, as indicated in Fig. 8) should be 2.5 ns (50 channels) longer than that for the pions and muons. These times of flight are shown in Fig. 13. The protons are well-separated from the pions and muons.

5. Summary

The new prototype LMRPCs have been built and tested both with cosmic rays and with test beams. The cosmic ray tests indicate a time resolution of ∼70 ps and a detection efficiency greater than 95% at a detector high voltage of ±6.3 kV. In the T963 beam test performed at FNAL, similar values of the detection efficiency and the time resolution were observed. The spatial

resolution of these LMRPCs along the direction of the read-out strips was near to or less than 1 cm. The performance of these LMRPC prototypes thus satisfies the requirements for the STAR MTD system, and also appears applicable for TOF at the electron ion collider eRHIC [11].

Acknowledgements

References

[1] M.C.S. Williams, E. Cerron, et al., Nucl. Instr. and Meth. A 434 (1999) 362.
[2] Chen Hong-Fang, Li Cheng, et al., High Energy Phys. Nucl. Phys. V26 N3 (2002) 201 (in Chinese).
[3] B. Bonner, H. Chen, G. Eppley, F. Geurts, J. Lamas-Valverde, Ch. Li, W.J. Llope, T. Nussbaum, E. Platner, J. Roberts, Nucl. Instr. and Meth. A 508 (2003) 181.
[4] Proposal for a Large-Area Time-of-Flight system for STAR, STAR-TOF Collaboration, May 2004, ⟨http://www.bonner-mac8.rice.edu/~TOF/TOF/Documents/TOF_20040524.pdf⟩.
[5] ALICE Time of Flight Addendum, CERN/LHCC 2002-016, Addendum to ALICE TDR 8, 24 April 2002.
[6] A new large-area muon telescope detector at mid-rapidity at RHIC, Division of Nuclear Physics Annual Meeting, Nashville, TN, USA, October 25–28, 2006.
[7] Zhangbu Xu, A novel and compact muon telescope detector for QCDLab, BNL LDRD project.
[8] Sun Yong-Jie, Li Cheng, et al., Nucl. Sci. Tech. V16 N4 (2005) 231.
[9] Huang Sheng-Li, Li Cheng, Xu, Zi-Zong, et al., High Energy Phys. Nucl. Phys. V27 N2 (2003) 154.
[10] Frank Simon, James Kelsey, Michael Kohl, Richard Majka, Miroslav Plesko, David Underwood, Tai Sakuma, Nikolai Smirnov, Harold Spinka, Bernd Surrow, arXiv:0711.3751.
[11] RHIC-II/eRHIC white paper (December 2006), ⟨http://www.bnl.gov/npp/docs/RHICplanning/rhic2_wp_draft_dec30_2006.pdf⟩.